Wearable Flexible Reconfigurable Antenna Integrated With Artificial Magnetic Conductor

Saud M. Saeed, *Student Member, IEEE*, Constantine A. Balanis, *Life Fellow, IEEE*, Craig R. Birtcher, Ahmet C. Durgun, *Member, IEEE*, and Hussein N. Shaman, *Member, IEEE*

***Abstract*—This letter presents a wearable flexible reconfigurable folded slot antenna. The antenna is composed of a folded slot and a stub where the reconfigurability is achieved by turning a p-i-n diode ON and OFF, which alters the radiation characteristics of the stub. The operating frequency and polarization of the slot and stub are different. Hence, a polarization-dependent dual-band artificial magnetic conductor (AMC) surface is integrated with the antenna to improve its radiation performance and to reduce the specific absorption rate (SAR). The antenna is designed and fabricated on a flexible substrate, and its performance is measured for both flat and curved configurations. The measurements show an excellent agreement with the simulations. To examine its performance as a wearable antenna, it is measured on a human body. Simulations show that the SAR level is reduced when the AMC surface is used as an isolator. The proposed wearable antenna structure can be used for wireless body area network (WBAN) and Worldwide Interoperability for Microwave Access (WiMAX) body-worn wireless devices.**

***Index Terms*—Artificial magnetic conductor (AMC), flexible antennas, folded slot antennas, reconfigurable antennas, wearable antennas.**

I. Introduction

WIRELESS body area network (WBAN) is an active research topic, especially in the healthcare area, as it provides cost-efficient and continuous monitoring of patients over a wide range of accessibility. In such a system, an array of body sensors is connected to a communication unit that collects the data and sends it to a health center [1]. This unit can either be located near or worn directly by the patient to minimize the impact on daily life activities. Hence, wearable antenna designs have attracted lots of interest as it can be utilized in similar on-body applications [2]–[8]. However, maintaining acceptable radiation characteristics with low levels of specific absorption rate (SAR) is a challenging task. In addition, antennas are preferred to be flexible and conformal to the human body [9]–[11]. The impact of the human body, which is considered as a lossy tissue, on the radiation efficiency is critical. Thus, it is recommended to use antennas that have unidirectional patterns, such as microstrips, or elements that have isolators to reduce the impact of the human body on their performance and to reduce the SAR level. Wearable antennas consisting of perfect electric conductors (PECs) are not preferred for low-profile applications due to the quarter-wavelength height required to increase the radiation efficiency [12], which increases the overall size and also makes the flexibility and reconfigurability of the antenna more challenging.

Artificial magnetic conductor (AMC) surfaces are being used as ground planes for low-profile applications, as discussed in [13]–[15]. Thus, an AMC surface can be used as an isolator in wearable antenna applications, and they have been reported in the literature [5]–[8]. In [5], a dual-band textile antenna operating at 2.45 and 5 GHz, which was printed on a dual-band electromagnetic bandgap substrate, was proposed. The back radiation was reduced by 10 dB, while the antenna gain increased by 3 dB. In [6], an inkjet-printed, low-profile, coplanar waveguide (CPW)-fed antenna was fabricated on a Jerusalem Cross AMC structure for bandwidth enhancement and SAR reduction. The front-to-back ratio and gain were increased by 8 and 3.7 dB, respectively, and a 64% reduction in SAR level was obtained. However, none of these antennas is reconfigurable.

In this letter, we are proposing a novel flexible reconfigurable antenna for a wearable remote patient monitoring system, where the data transfer between the communication unit, the sensors, and the health center is performed over WBAN and Worldwide Interoperability for Microwave Access (WiMAX) bands, respectively. The reconfigurable antenna does not require a complex bias circuitry, and it radiates orthogonally polarized waves in the WBAN and WiMAX bands, which provides extra isolation. The SAR level is significantly reduced by the use of the dual-band, polarization-dependent AMC surface.

II. Antenna and AMC Surface Design

The antenna element used in this letter consists of three parts: a 50-Ω CPW feedline, a slot, and a stub, as shown in Fig. 1; the operating principles were reported in [11]. The folded slot antenna resonates at a single band when its circumference is equal to one-guided wavelength. The stub is used to match the high impedance of the slot to the 50-Ω CPW feedline. If the stub is symmetrical with respect to the CPW feedline, it does not radiate and the antenna has a single operating frequency. However,

Manuscript received May 19, 2017; accepted June 18, 2017. Date of publication June 27, 2017; date of current version August 21, 2017. This work was supported in part by a research contract between Arizona State University and King Abdulaziz City for Science and Technology. *(Corresponding author: Constantine A. Balanis.)*

S. M. Saeed is with the School of Electrical, Computer and Energy Engineering, Arizona State University, Tempe, AZ 85287 USA, and also with the College of Engineering, Prince Sattam Bin Abdulaziz University, Al-Kharj 16278, Saudi Arabia (e-mail: smsaeed@asu.edu).

C. A. Balanis and C. R. Birtcher are with the School of Electrical, Computer and Energy Engineering, Arizona State University, Tempe, AZ 85287 USA (e-mail: balanis@asu.edu; craig.birtcher@asu.edu).

A. C. Durgun is with the Intel Corporation, Chandler, AZ 85226 USA (e-mail: ahmet.c.durgun@intel.com).

H. N. Shaman is with the National Center for Sensors and Defense Systems Technologies, King Abdulaziz City for Science and Technology, Riyadh 12371, Saudi Arabia (e-mail: hshaman@kacst.edu.sa).

Color versions of one or more of the figures in this letter are available online at http://ieeexplore.ieee.org.

Digital Object Identifier 10.1109/LAWP.2017.2720558

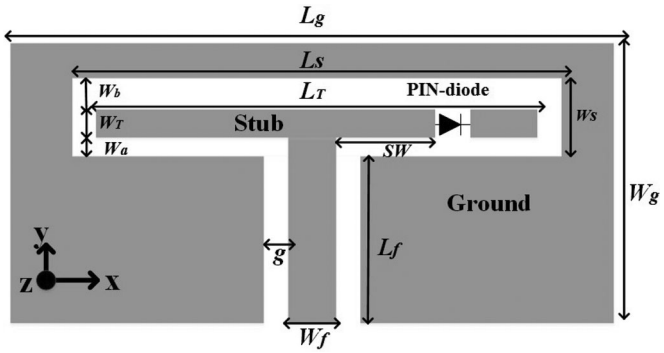

Fig. 1. Reconfigurable folded slot antenna. Dimensions: $W_g = 89$ mm, $L_g = 83$ mm, $W_s = 5.3$ mm, $L_s = 51$ mm, $W_T = 0.8$ mm, $L_T = 50$ mm, $W_f = 3.6$ mm, $L_f = 46$ mm, $g = 0.2$ mm, $W_a = 0.5$ mm, $W_b = 4$ mm, and SW$= 8$ mm.

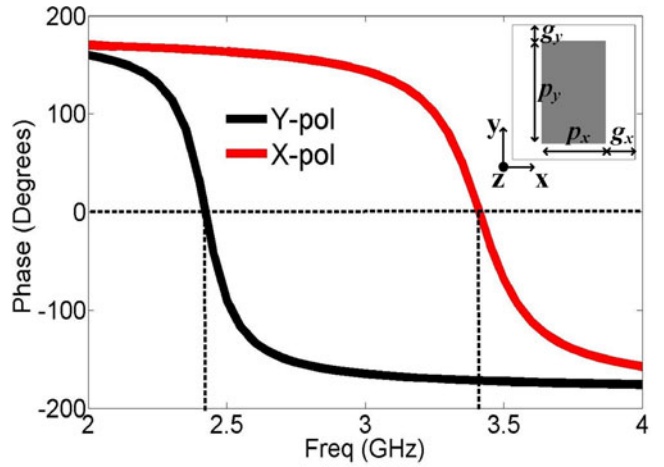

Fig. 2. Reflection phase of a rectangular patch unit cell of the AMC surface. Dimensions: $p_y = 29$ mm, $p_x = 23$ mm, $g_y = 0.5$ mm, and $g_x = 3$ mm.

if the stub is asymmetrical with respect to the feedline, then the current on the stub is redirected resulting in a dipole-type radiation. Thus, the folded slot antenna can be reconfigured by changing the length of the stub. This can be achieved by utilizing a p-i-n diode, and turning it ON and OFF, with the aid of a simple bias circuitry, as discussed in [11]. If the diode is OFF, both the slot and the stub resonate with orthogonal polarizations, according to Babinet's principle [12]. Based on the coordinate system of Fig. 1, the slot is *y*-polarized while the stub is *x*-polarized.

To reduce the backward radiation and lower the SAR level, the antenna is placed on an AMC surface, which considerably lowers the profile of the entire structure, compared to a PEC. Since the antenna has two operating bands with orthogonal polarizations, the AMC surface should also have two separate bands with different polarizations. To achieve this, a rectangular patch is utilized as the unit cell of the AMC, as shown in Fig. 2. The AMC has a zero reflection phase at 2.4 and 3.4 GHz for *y*- and *x*-polarized normal incident plane waves, respectively. The AMC surface consists of nine unit cells (3×3), as depicted in Fig. 3(a), to maintain a compact size and a reasonably low backward radiation. The total size of the structure measures approximately $0.71\lambda \times 0.66\lambda$ at 2.4 GHz.

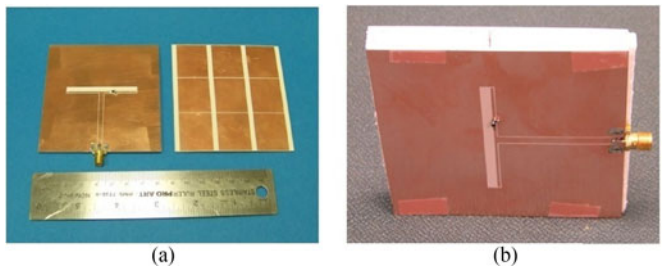

Fig. 3. Fabricated prototypes. (a) Antenna and AMC surface. (b) Entire antenna structure.

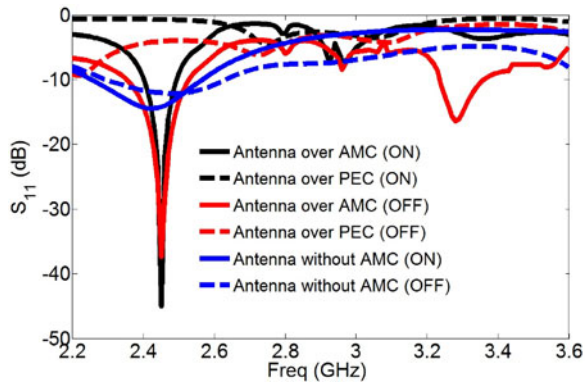

Fig. 4. Simulated reflection coefficients of the proposed antenna with and without the (AMC/PEC) surfaces.

The entire structure consists of three layers: the flexible reconfigurable antenna on top, the AMC surface on the bottom, and a flexible foam material in between. Both the antenna and the AMC were fabricated, using an etching process, on Rogers RO3003 flexible substrate, with a dielectric constant and a loss tangent of 3 and 0.0013, respectively; the thickness of the substrate was 1.52 mm. The fabricated prototype of the proposed antenna structure is displayed in Fig. 3(a) and (b).

Unlike a wire dipole, the CPW-fed folded slot antenna has a ground plane around the slot, and if it is backed by an AMC surface, the coupling between the ground plane and the AMC may decrease the radiation efficiency and change the impedance matching of the antenna. Hence, the antenna geometry and its height should be optimized to minimize the coupling and maintain good impedance matching. The antenna is placed, approximately $\lambda/20$ at 2.4 GHz, above the AMC surface, and a flexible foam material is used to fill the space between the radiating element and the AMC surface. The High Frequency Structural Simulator (HFSS) is used to design and simulate the entire antenna structure. Fig. 4 shows the simulated S_{11} for different states of the p-i-n diode (ON/OFF) and with and without the (AMC/PEC) surfaces. It is observed that the matching is better when the AMC surface is used instead of the PEC.

III. Results and Discussion

To examine the performance of the proposed wearable antenna backed by an AMC surface, the radiation characteristics, such as the reflection coefficient (S_{11}) and the radiation patterns, were measured and compared to the predicted results. In Fig. 5, a comparison between measured and simulated S_{11} of

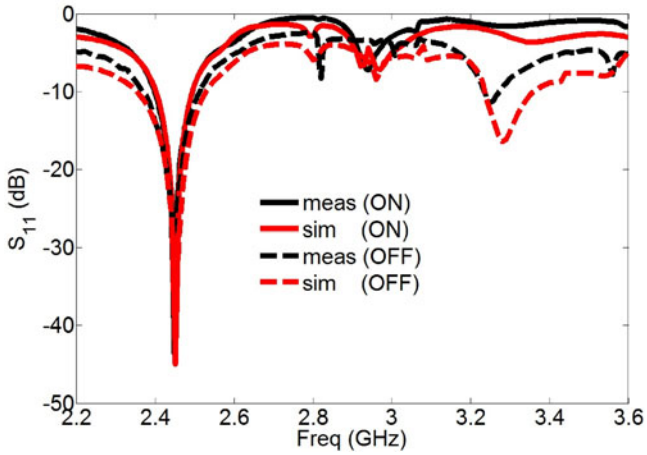

Fig. 5. Measured and simulated reflection coefficients of the proposed antenna structure for different states of the p-i-n diode (ON/OFF).

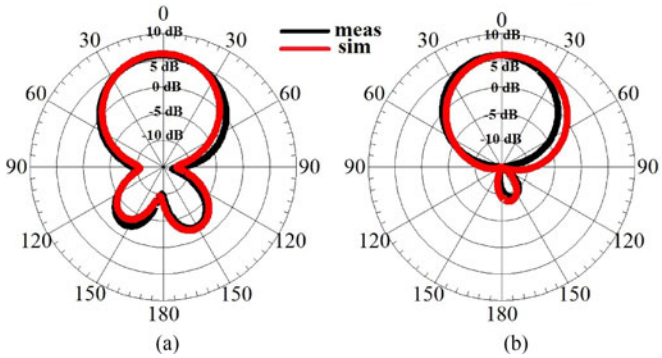

Fig. 6. Measured and simulated radiation patterns of the proposed structure at 2.45 GHz (diode is OFF): (a) E-plane. (b) H-plane.

the proposed structure for different states of the p-i-n diode is displayed; an excellent agreement is achieved between simulations and measurements. If the p-i-n diode is ON, the proposed antenna structure is single-band from the slot, and it works at 2.45 GHz with a −10-dB measured impedance bandwidth of 0.1 GHz (2.4–2.5 GHz) for WBAN applications of wearable devices. However, if the p-i-n diode is OFF, the antenna structure is dual-band from the slot at 2.45 GHz with a −10-dB measured impedance bandwidth of 0.17 GHz (2.35–2.52 GHz), and the stub at 3.3 GHz with a −10-dB measured impedance bandwidth of 0.1 GHz (3.28–3.38 GHz). In this case, the antenna can be used for both WBAN and WiMAX wireless applications. The measured and simulated radiation patterns (OFF case) of the flat configuration of the proposed structure are displayed in Figs. 6 and 7. Similar patterns are obtained at 2.45 GHz when the p-i-n diode is activated (ON). It is clear that the AMC surface, reduces the back radiation, which will result in the SAR level reduction. Table I lists a comparison between the gains at broadside ($\theta = 0$), with and without the AMC surface. It is observed that with the AMC surface, the gain of the antenna is enhanced by about 3.6 dB for the slot and 2.4 dB for the stub configurations. It should be mentioned that if a larger AMC surface (more unit cells) is used, the antenna gain can be increased with further reduction in the back radiation. However, this will increase the overall size, which is not preferred.

For wearable applications, the flexibility test of the antenna is required to ensure that it can be worn or conformed on a

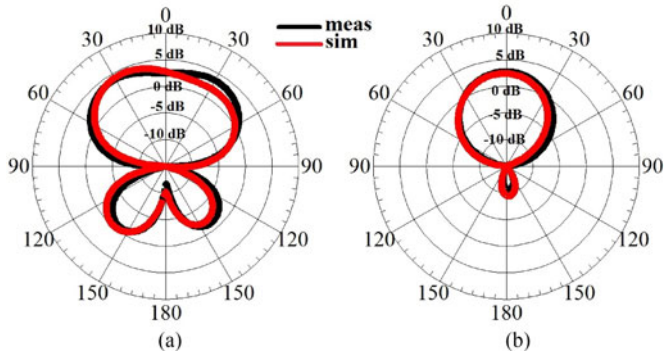

Fig. 7. Measured and simulated radiation patterns of the proposed structure at 3.3 GHz (diode is OFF): (a) E-plane. (b) H-plane.

TABLE I
GAIN COMPARISON BETWEEN THE ANTENNA WITH/WITHOUT THE AMC SURFACE

Frequency	Antenna Without AMC Gain (dB)	Antenna With AMC Gain (dB)
On (2.45 GHz)	2.7	6.4
Off (2.45 GHz)	2.6	6.2
Off (3.3 GHz)	0.6	3.0

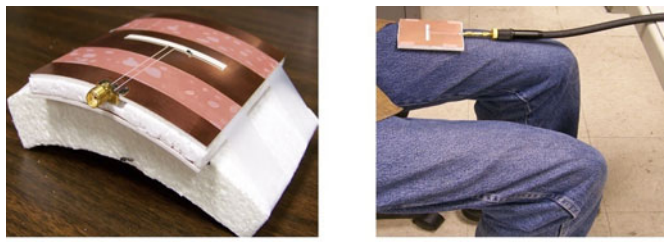

Fig. 8. Fabricated prototypes. (a) Curved antenna structure. (b) Antenna structure placed on human body.

human body. Fig. 8 illustrates the antenna when it is curved and mounted on a human body (leg). To ensure that the proposed antenna maintains its resonant frequencies when it is bent or conformed on a curved structure, it was tested for the reflection coefficients of the curved structure and compared to the reflection coefficients of the flat configuration. The comparison is displayed in Fig. 9, which indicates that the resonant frequencies for both flat and curved configurations are the same. The wearability of the proposed antenna, when it is mounted on human body tissue, as shown in Fig. 8(b), must be examined to test the impedance mismatch due the impact of human body tissue on its performance. The measured reflection coefficients are also shown in Fig. 9 for different states (ON/OFF) of the p-i-n diode; the antenna maintains its resonant frequencies for both WBAN and WiMAX applications.

Another performance metric is the SAR level, which is a factor or a standard that represents the amount of electromagnetic power absorbed by the human body. According to the Federal Communications Commission, the standard value of SAR level is about 1.6 W/kg in 1 g of tissue [16]. The fundamental equation of calculating the SAR level is shown as follows, where σ is the conductivity, ρ is the mass density of the tissue, and E is the

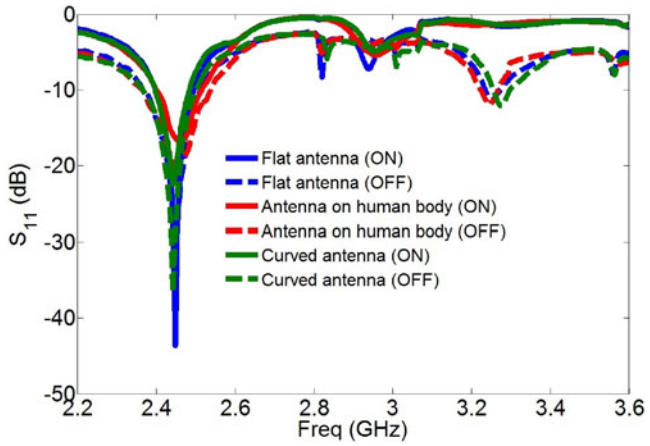

Fig. 9. Measured reflection coefficients of the proposed antenna structure for different configurations: flat, curved, and antenna on human body (leg).

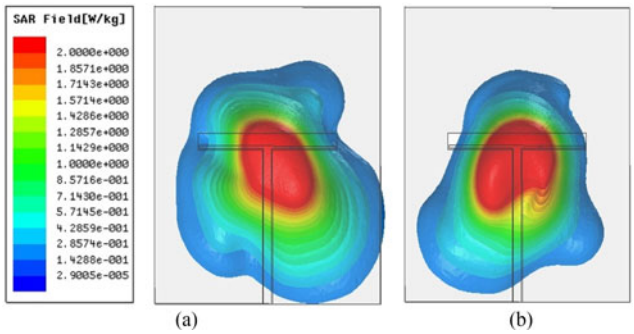

Fig. 10. Averaged SAR values of the antenna without AMC surface (diode is OFF): (a) SAR at 2.45 GHz. (b) SAR at 3.3 GHz.

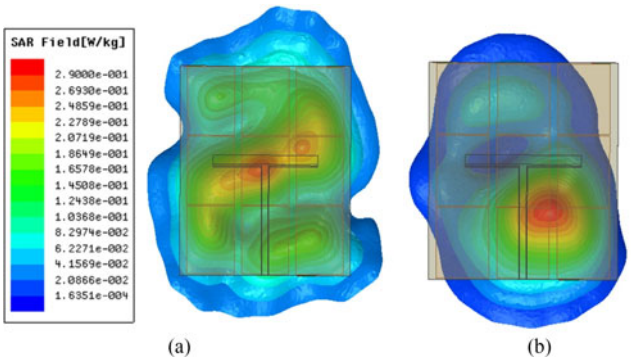

Fig. 11. Averaged SAR values of the proposed antenna structure with AMC surface (diode is OFF): (a) SAR at 2.45 GHz. (b) SAR at 3.3 GHz.

electric field [16]:

$$\mathrm{SAR} = \frac{\sigma |E^2|}{\rho}. \tag{1}$$

The SAR level of the proposed antenna was examined by modeling a human head in the HFSS as a sphere with a dielectric constant (ϵ_r) of 39.2, a conductivity (σ) of 1.8 S/m, and a mass density of 1000 kg/m^3 [16]. The accepted power by the antenna is about 0.1 W, and the distance between the antenna (with/without the AMC surface) and the human head is about 1 mm. Fig. 10 shows the averaged SAR values over 1 g without the AMC surface, when the diode is OFF and the antenna resonates at 2.45 and 3.3 GHz. It is clear that the SAR is above 1.6 W/kg, which is not preferred for wearable applications. Fig. 11 displays the averaged SAR values over 1 g with the presence of the AMC surface; it is evident that a significant SAR reduction is obtained by using the AMC surface. According to the scale in Figs. 10 and 11, the maximum SAR value is reduced from 2 to 0.29 W/kg.

IV. Conclusion

A novel antenna design that merges the flexibility, reconfigurability, and wearability of antennas in one design is proposed. The flexible reconfigurable antenna has either single or dual bands with two orthogonal polarizations. It is integrated with a polarization-dependent AMC surface that also has dual-band reflection phase with two orthogonal polarizations. The proposed design is tested for flat and curved configurations, and it is measured on a human body. It is observed that it maintains its performance and has excellent radiation characteristics; the SAR level is reduced after using the AMC.

References

[1] D. P. Tobn, T. H. Falk, and M. Maier, "Context awareness in WBANs: A survey on medical and non-medical applications," *IEEE Wireless Commun.*, vol. 20, no. 4, pp. 30–37, Aug. 2013.

[2] G. A. Conway and W. G. Scanlon, "Antennas for over-body-surface communication at 2.45 GHz," *IEEE Trans. Antennas Propag.*, vol. 57, no. 4, pp. 844–855, Apr. 2009.

[3] K. Koski, L. Sydnheimo, Y. Rahmat-Samii, and L. Ukkonen, "Fundamental characteristics of electro-textiles in wearable UHF RFID patch antennas for body-centric sensing systems," *IEEE Trans. Antennas Propag.*, vol. 62, no. 12, pp. 6454–6462, Dec. 2014.

[4] B. Hu, G. P. Gao, L. L. He, X. D. Cong, and J. N. Zhao, "Bending and on-arm effects on a wearable antenna for 2.45 GHz body area network," *IEEE Antennas Wireless Propag. Lett.*, vol. 15, pp. 378–381, 2016.

[5] S. Zhu and R. Langley, "Dual-band wearable textile antenna on an EBG substrate," *IEEE Trans. Antennas Propag.*, vol. 57, no. 4, pp. 926–935, Apr. 2009.

[6] H. R. Raad, A. I. Abbosh, H. M. Al-Rizzo, and D. G. Rucker, "Flexible and compact AMC based antenna for telemedicine applications," *IEEE Trans. Antennas Propag.*, vol. 61, no. 2, pp. 524–531, Feb. 2013.

[7] S. Yan, P. J. Soh, and G. A. E. Vandenbosch, "Low-profile dual-band textile antenna with artificial magnetic conductor plane," *IEEE Trans. Antennas Propag.*, vol. 62, no. 12, pp. 6487–6490, Dec. 2014.

[8] B. S. Cook and A. Shamim, "Utilizing wideband AMC structures for high-gain inkjet-printed antennas on lossy paper substrate," *IEEE Antennas Wireless Propag. Lett.*, vol. 12, pp. 76–79, 2013.

[9] H. R. Khaleel, H. M. Al-Rizzo, and A. I. Abbosh, "Design, fabrication, and testing of flexible antennas," in *Advancement in Microstrip Antennas With Recent Applications*, A. Kishk, Ed. Vienna, Austria: InTech, 2013.

[10] A. C. Durgun, C. A. Balanis, C. R. Birtcher, and D. R. Allee, "Design, simulation, fabrication and testing of flexible bow-tie antennas," *IEEE Trans. Antennas Propag.*, vol. 59, no. 12, pp. 4425–4435, Dec. 2011.

[11] S. M. Saeed, C. A. Balanis, and C. R. Birtcher, "Inkjet-printed flexible reconfigurable antenna for conformal WLAN/WiMAX wireless devices," *IEEE Antennas Wireless Propag. Lett.*, vol. 15, pp. 1979–1982, 2016.

[12] C. A. Balanis, *Antenna Theory: Analysis and Design*, 4th ed. Hoboken, NJ, USA: Wiley, 2016.

[13] D. Sievenpiper, "High-impedance electromagnetic surfaces," Ph.D. dissertation, Dept. Elect. Eng., UCLA, Los Angeles, CA, USA, 1999.

[14] C. A. Balanis, *Advanced Engineering Electromagnetics*, 2nd ed., Hoboken, NJ, USA: Wiley, 2012.

[15] Y. Fan and Y. Rahmat-Samii, "Reflection phase characterizations of the EBG ground plane for low profile wire antenna applications," *IEEE Trans. Antennas Propag.*, vol. 51, no. 10, pp. 2691–2703, Oct. 2003.

[16] *IEEE Recommended Practice for Determining the Peak Spatial-Average Specific Absorption Rate (SAR) in the Human Head From Wireless Communications Devices: Measurement Techniques—Redline*, IEEE Std 1528-2013 (Revision of IEEE Std 1528-2003)—Redline, Sep. 2013, pp. 1–500.